The Role of Stiffness in Versatile Robotic Grasping

Christopher J. Stabile, David J. Levine, Gokulanand M. Iyer, Carmel Majidi, and Kevin T. Turner

Abstract—Traditionally, robotic grippers are based on stiff materials, enabling end effectors with high load capacity and precision for industrial applications. Recent advances in soft robotics have led to a proliferation of novel gripper designs with increased conformability to accommodate objects of varying shape, size, material, and surface properties, allowing for grippers that can safely manipulate a wide range of objects. While compliant materials offer noted advantages for robotic grasping, their ability to deform limits their load capacity. Therefore, stiffness selection is critical in gripper design, and the use of materials with tunable stiffness can be exploited for new functionality. Here, we present a mechanics-based investigation of the design of versatile grippers that can accommodate both soft and stiff grasping modalities. We examine the ability to form contact and how different types of gripping forces, including frictional, normal, and adhesive interactions, can be leveraged and controlled. We use analytical models based on elastic beam theory and contact mechanics to quantify the relationship between gripper deflection, contact area, contact pressure, and load capacity. We then use these models to define quantitative conditions for successful grasping as a function of the geometry of the object and the stiffness and geometry of the gripper. Finally, we conclude with an experimental case study and a discussion of how stiffness can be selected and modulated to realize successful grasping for different classes of objects.

Index Terms—Soft robot materials and design, soft robot applications, grasping.

I. INTRODUCTION

S a result of recent advances in materials, soft robotics, and stretchable electronics, the range and capabilities of robotic grasping technologies have been rapidly expanding [1]. Traditionally, robotic grippers are made of stiff components (materials with $E>10^6$ kPa) that can rotate or translate using joints, enabling end-effectors with high load capacity and precision for industrial applications. However, these grippers lack the

Manuscript received September 8, 2021; accepted January 20, 2022. Date of publication February 7, 2022; date of current version March 2, 2022. This letter was recommended for publication by Associate Editor M. Calisti and Editor K.-J. Cho upon evaluation of the reviewers' comments. This work was supported in part by the National Science Foundation under the National Robotics Initiative through Award #1830475 and in part by the University of Pennsylvania through Award #1830362 at Carnegie Mellon University. (Christopher J. Stabile, David J. Levine, and Gokulanand M. Iyer contributed equally to this work.) (Corresponding author: Kevin T. Turner.)

Christopher J. Stabile, David J. Levine, Gokulanand M. Iyer, and Kevin T. Turner are with the Department of Mechanical Engineering & Applied Mechanics, University of Pennsylvania, Philadelphia, PA 19104 USA (e-mail: cstabile@seas.upenn.edu; djlev@seas.upenn.edu; giyer@seas.upenn.edu; kturner@seas.upenn.edu).

Carmel Majidi is with the Department of Mechanical Engineering, Carnegie Mellon University, Pittsburgh, PA 15213 USA (e-mail: cma-jidi@andrew.cmu.edu).

This letter has supplementary downloadable material available at https://doi.org/10.1109/LRA.2022.3149036, provided by the authors. Digital Object Identifier 10.1109/LRA.2022.3149036

compliance necessary for safe and reliable operation in human environments, and cannot successfully grasp diverse objects of varying shape, size, material, and surface properties [2], [3]. In addition, contact between a rigid manipulator and an object can lead to object damage or undesired object trajectories during an attempted grasp. Complex control schemes are often implemented to avoid this problem [4]. In contrast, underactuated, rigid robotic grippers can passively conform to unknown objects, and the compliance can be carefully selected to grasp diverse object sets [5], [6]. However, these grippers lack the ability to continuously deform within the bulk of each finger, which can aid grasping in many scenarios [2].

To solve this, recent advances in soft robotics have led to a proliferation of novel gripper designs with increased conformability via bending and bulk deformation to facilitate grasping in unstructured applications such as manufacturing, prosthetics, search and rescue, and exploration [7]. The use of soft materials in grippers significantly reduces design complexity, weight, and cost, as compliant materials can passively conform to an object's shape. The material and geometry of the end effector will determine its mechanical compliance, which directly impacts how it interacts with its surroundings. While compliant materials offer advantages for robotic grasping, their compliance limits load capacity. Thus, the selection of stiffness is critical in the performance of any gripper and needs to be carefully considered in design. Moreover, the use of materials with tunable stiffness (i.e., tunable rigidity) that can be actively switched between soft and stiff states offer possibilities for expanding gripper capabilities.

Tunable stiffness materials [8]-[10] have been successfully implemented for use in robotic grippers [2]. By switching between soft and stiff states, these materials can alter the dominant forces that control grasping. Several approaches can be used for active stiffness change, including phase-change materials [11]-[13], electroadhesives [14], and particle jamming systems [15]. Stiffness change can be triggered globally throughout the volume of an entire end-effector, allowing for full envelopment of a target object to maximize grasp success [15]. Alternatively, stiffness can be tuned locally at specific locations within an end-effector to enable different types of object grasps, such as caging or pinching, which may be suitable for objects of different sizes [16]. Caging grasps are common to soft end-effectors capable of distributed, continuous actuation, while rigid grippers are more suited for pinching grasps. With tunable stiffness, a single end-effector design can achieve both grasping modalities. Therefore, grippers comprised of materials with tunable stiffness can grasp wider classes of objects with greater success, while minimizing the total number of parts required for successful

2377-3766 © 2022 IEEE. Personal use is permitted, but republication/redistribution requires IEEE permission. See https://www.ieee.org/publications/rights/index.html for more information.

operation. Currently, there is a lack of succinct, quantitative conditions for grasp feasibility, and scant knowledge of the effects of gripper stiffness on grasp success. In order to successfully design versatile grippers that utilize stiffness changes to interact with a wide class of objects, there is a need to establish (1) quantitative conditions for grasp feasibility, and (2) mechanics-based grasping models that quantify the effect of stiffness on the type and magnitude of gripping forces present during a given grasp.

In this paper, we present a mechanics-based investigation of gripper stiffness and its effect on gripper versatility. We examine the ability to form contact and how different types of gripping forces, including frictional, supportive and adhesive interactions, can be exploited. To assess gripper designs with different stiffnesses, we use analytical models based on beam theory and contact mechanics to quantify the relationship between gripper deflection, contact area, contact pressure, and load capacity. We then use these models in conjunction with quantitative conditions for grasp feasibility to map the effect of the geometry of the object and gripper, the stiffness, and grasping configuration on grasp success.

Our analysis is divided into two parts. We first investigate the effect of stiffness modulation on grasp feasibility, and then investigate the effect of stiffness changes on the formation of contact area and pressure between a gripper and an object. Finally, we conclude with a discussion of our results and stiffness modulation strategies to promote grasp success for different classes of objects.

II. THEORETICAL FORMULATION & RESULTS

A. Effect of Gripper Stiffness on Grasp Feasibility

In order to guide the design of versatile grippers, there is a need for generalized, analytical models that can predict the behavior of soft actuators, especially those with tunable properties. While numerical analyses can be used to evaluate a gripper's behavior (e.g., deformation, force output), they are computationally expensive, particularly when accounting for contact with an object. Therefore, a simple model that can relate a gripper's geometry and material composition to contact forces in a prescribed object space and provide quantitative conditions for grasp feasibility would be useful for soft gripper design and help guide the integration of tunable stiffness materials into grasping systems. To achieve this, we extend and apply the model from Zhou *et al.* [17], and focus our analysis on fingered gripper designs.

We examine the case of contact between a two-fingered gripper and a rigid cylindrical object. Due to symmetry, only half of the system is modeled, as shown in Fig. 1. The finger is modeled as an inextensible, flexible, 2-D elastic rod with length L, flexural rigidity D, mass per unit length ρ , uniform intrinsic curvature profile κ_0 , and a fingertip with radius R_f . The object is defined as a rigid cylinder with radius R_o and mass 2M. The fingertip contacts the object at a location defined by the angle β , with the object's center located at a horizontal distance S and a vertical distance S from the gripper's clamped end. The gripper's centerline is parameterized by the arc length variable S0. The variable S1. The variable S3 describes the finger's shape, or

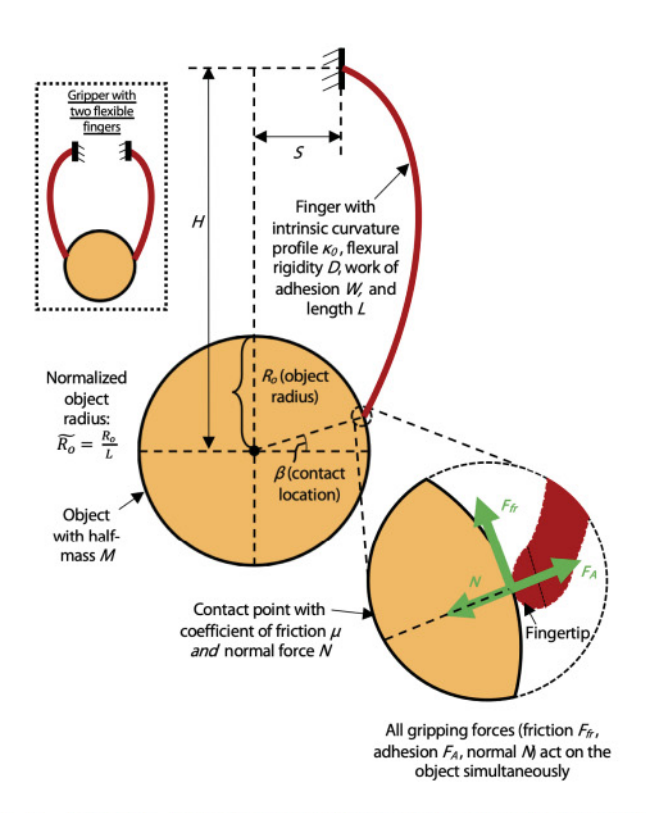


Fig. 1. Schematic describing contact between a two-fingered gripper and a cylindrical object. Symmetry is employed and thus we only include one finger. The enlarged view shows the gripping forces present at the contact, including frictional, normal, and adhesive loads.

the angle between the unit tangent at every location along the gripper's centerline and the unit horizontal. We consider three different forces during a grasp: frictional, normal, and adhesive forces. By considering a cylindrical object we are able to vary the vertical components of the friction, adhesion, and normal forces through the variation of a single parameter, β . For an object of arbitrary geometry, and assuming a small contact area relative to the local radius of curvature, the magnitudes of the vertical components of the three forces will still depend on the location of contact, but the dependence will be different as compared to a cylindrical object.

The total potential energy associated with bending the finger into contact with the object is

$$V = \int_0^L \left\{ \frac{D}{2} (\theta' - \kappa_0)^2 + \rho g(L - s) \sin \theta(s) - F_l \cdot r' \right\} ds$$

where F_l is the terminal load vector ($F_l = Nu_1 + F_{fr}u_2$, where u_1 and u_2 are the unit normal and unit tangent to the object, respectively) and r' is the unit tangent to the gripper's centerline [17]. Minimization of V gives the governing equation for the elastic finger as

$$D(\theta'' - \kappa_0') - \rho g(L - s)\cos\theta + F_y\cos\theta - F_x\sin\theta = 0.$$
(2)

The solution to the differential equation must satisfy the boundary conditions: $\theta(0) = 0$ and $\theta'(0) = 0$. Here, F_x and F_y are the horizontal and vertical components of the total contact

force. These components are given by

$$F_x = N\cos\beta + F_{fr}\sin\beta \tag{3}$$

$$F_u = -N\sin\beta + F_{fr}\cos\beta \tag{4}$$

where N is the normal force acting perpendicular to the contact and F_{fr} is the friction force acting tangent to the contact. The friction force is defined as

$$F_{fr} = \begin{cases} \frac{-Mg + F_A \sin \beta}{\cos \beta} &, \quad \beta > 0 \\ -Mg &, \quad \beta = 0 \\ \frac{-Mg + N \sin \beta}{\cos \beta} &, \quad \beta < 0 \end{cases}$$
(5)

where F_A is the force due to adhesion between the gripper and the object. Modeling adhesion between objects can be challenging, but for many soft systems, the adhesive pull-off force can be well described by the traditional JKR model [18]. The JKR model gives the adhesive force as

$$F_A = \frac{3}{2}\pi W_{adh}R\tag{6}$$

where W_{adh} is the work of adhesion between the object and gripper, and R is the equivalent radius of contact.

To utilize this model to understand the feasibility of a grasp, we vary β and R_o and prescribe κ_0 , D, S and M. For each combination of β and R_o , we solve (2) for the force required to bend the gripper from its uniform intrinsic curvature profile κ_0 into contact to overcome the object's weight (and lift). The force required to bend the gripper into contact is assumed to be fully transmitted to the object. From this, we calculate the normal force, N, and the required frictional force, F_{fr} , for a range of gripping locations and object radii. To assess whether or not a given grasp configuration is feasible, we enforce restrictions on the normal force and the coefficient of friction required to lift the object (assuming Coulomb friction, with $\mu \geq F_{fr}/N$). These restrictions are set by the types of materials and actuators commonly used in grasping systems. The two constraints for grasp feasibility that we impose are N < 0.1 N or N < 10 N, and μ_{\min} < 1. The normal force bounds are based on reported normal force capacities of grippers from the literature [2], [3], [17], [19], [20]. Two different upper bounds are used since the force output of grippers with high and low flexural rigidities can differ drastically, and the allowable normal force depends on the application and object set. Meanwhile, the coefficient of friction at an interface depends on the material properties of both the gripper and the object. In our analysis, a grasp is considered infeasible if the required friction coefficient, calculated as F_{fr}/N , is larger than a reasonable value. We selected this bound on the coefficient of friction because many contacts in soft grasping scenarios are mixed-material systems, where the friction coefficient is often in the range of 1 to 1.2 [21], but this value can be changed for different material combinations, as we do in our experiments. We also note that our assumption of Coulomb friction may underestimate the overall friction force produced at soft contacts, but such interactions lie outside the scope of the presented analysis. When enforcing the constraints

on the normal force and the coefficient of friction, two distinct regions are generated: a region where grasping is infeasible, marked in orange, and a region where grasping and lifting is feasible, marked in blue, as shown in the grasp feasibility plots in the Discussion section. To assess grippers with different flexural rigidities, we solve (2) for a range of β and R_o values for grippers with low and high flexural rigidities varying by a factor of $100 \times$ $(\ddot{D} = 0.4, 40)$ and for objects of varying mass, differing by a factor of $3 \times$ to $30 \times$ (M = 0.2, 0.6, 6). We do not assume a particular technology to be the driving method for modulating D, although different approaches for stiffness modulation will lead to different grasping behaviors and must be carefully selected for a desired set of objects [9], [10]. In this model, we use normalized versions of all variables, which include $\tilde{D} = \frac{D}{\rho g L^3}$, $\tilde{M} = \frac{M}{\rho L}$, $\tilde{R_o}=rac{R_o}{L}, \tilde{N}=rac{N}{
ho g L},$ and $\tilde{\kappa_0}=\kappa_0 \, L$ with L=55 mm and linear density $\rho = 0.31 \,\text{kg/m}$ averaged from grippers sourced from the literature [2], [3], [17], [19], [20]. Other methods, such as grasp stiffness matrices [22], [23] and force closure analyses [24], have been used to examine the effect of gripper stiffness and materials selection on grasp stability, or the ability of a gripper to hold an object subject to a small external disturbance. However, in our approach, we assess grasp feasibility for a set of factors in gripper design that grasp stability analyses overlook. These factors include: (1) the ability of the gripper's contact interface to provide the necessary friction to hold an object, (2) the gripper's ability to damage an object, or (3) any adhesive forces present at the contact.

B. Effect of Gripper Stiffness on Contact Area and Pressure

When a finger-like gripper contacts an object, the gripper deforms through bending of the finger and bulk deformation in the vicinity of the contact. The relative amount of bending to bulk deformation is a function of the properties of the gripper and the object. The bulk deformation of the gripper and object results in a finite contact area over which the gripper applies pressure to the object. An analytical model is developed here to predict, for small displacements, the contact area and pressure at the contact between a finger-like gripper with a rectangular cross section and a cylindrical object, as depicted in Fig. 2. This model illustrates the effect of gripper geometry and modulus on the contact area and pressure formed with an object during grasping. Depending on the object being grasped, the required or allowable contact area and pressure will vary. Therefore, this model can inform gripper design, including the use of materials with tunable stiffness, as well as gripper positioning during grasping.

The gripper is modeled as a cantilever beam with length L, height h, depth b, Young's modulus E_g , and Poisson's ratio ν_g . The object is modeled as a cylinder with radius R, depth $b_o > b$, Young's modulus E_o , and Poisson's ratio ν_o . The gripper initially makes point contact with the object at a distance $x = L_c$ from the clamped end and is then displaced into further contact through an applied displacement d. For a small displacement d, it is assumed that a contact force F acts perpendicular to the contact at $x = L_c$. In the deformed finger, there is strain energy

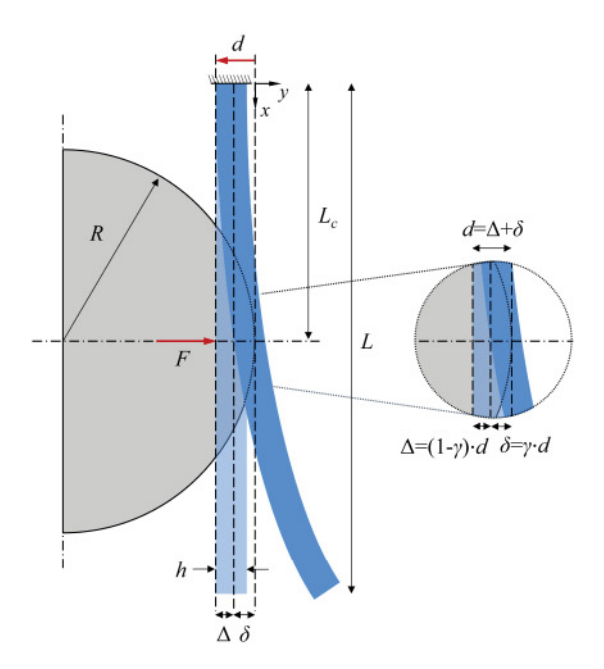


Fig. 2. Schematic of the contact between a finger-like gripper, modeled as a cantilever beam, and a cylindrical object. The beam initially makes contact at a point with the object at a distance L_c from the clamped end before being moved by displacement d, resulting in indentation depth δ and beam deflection Δ . Due to symmetry, only one finger of the two-finger gripper and half of the cylindrical object are modeled.

due to bending

$$U_{bend} = \int_0^{L_c} \frac{M^2}{2E_o I} dx = \frac{F^2 L_c^3}{6E_o I},\tag{7}$$

where I is the area moment of inertia of the beam cross-section and the contact force can be expressed as a function of beam deflection Δ :

$$F = \frac{3E_g I \Delta}{L_c^3}. (8)$$

Assuming Hertzian contact between cylinders with parallel axes, the contact force can be expressed as a function of the indentation depth δ as

$$F \approx \frac{\pi}{4} E^* b \delta,$$
 (9)

where $E^* = [(1 - \nu_o^2)/E_o + (1 - \nu_g^2)/E_g]^{-1}$. The elastic strain energy associated with contact deformation is

$$U_{contact} = \int_0^{\delta} F d\delta' = \frac{\pi}{8} E^* b \delta^2.$$
 (10)

Therefore, the total elastic strain energy due to bending and contact deformation is

$$U_{tot} = U_{bend} + U_{contact} = \frac{F^2 L_c^3}{6E_o I} + \frac{\pi}{8} E^* b \delta^2.$$
 (11)

For an applied displacement d of the clamped end of the beam, there will be a beam deflection Δ and indentation depth δ that sum to the applied displacement. By defining the indentation depth as a fraction γ of the applied displacement, δ is expressed

as

$$\delta = \gamma d = d - \Delta. \tag{12}$$

Substituting (8) and (12) into (11) and minimizing the total potential energy with respect to indentation depth as $dU_{tot}/d\delta = 0$, while assuming a rectangular cross-section with $I = bh^3/12$, leads to

$$\gamma = \frac{(1/\pi)(E_g/E^*)(h/L_c)^3}{(1/\pi)(E_g/E^*)(h/L_c)^3 + 1}.$$
 (13)

The half-width of the contact is given by $a = \sqrt{\delta R}$, and thus

$$\frac{a}{R} = \sqrt{\gamma} \sqrt{\frac{d}{R}}.$$
 (14)

Finally, assuming a parabolic contact pressure distribution of the form $P(x)=(-C_1x^2+C_2)/b$ and applying the conditions $P(\pm a)=0$ and $F=2b\int_0^a P(x)dx$ the contact pressure distribution is obtained as

$$P(x) = -\frac{3\pi}{16}E^*\frac{a}{R}\left[\left(\frac{x}{a}\right)^2 - 1\right],\tag{15}$$

and maximum contact pressure $(P_{max} = P(0))$ of

$$P_{\text{max}} = \frac{3\pi}{16} E^* \frac{a}{R},\tag{16}$$

and average contact pressure $P_{avg} = \frac{1}{a} \int_0^a P(x) dx$ of

$$P_{avg} = \frac{\pi}{8} E^* \frac{a}{R} = \frac{2}{3} P_{max}.$$
 (17)

From (13), it is evident that the relative amount of contact and bending deformation depends on the non-dimensional parameters E_g/E^* and h/L_c , where E_g/E^* is the ratio of beam modulus to contact modulus and h/L_c is the ratio of beam thickness to effective beam length. From (14), it is seen that the normalized half-width of the contact a/R depends on γ and d/R. As the beam modulus increases or the contact modulus decreases, γ increases and a greater fraction of the applied displacement is accommodated through bulk contact deformation, as opposed to beam deflection. Additionally, γ increases as the beam thickness increases, or the effective beam length decreases (i.e., contact occurs closer to the clamped end). Since the amount of bulk deformation increases with γ , the size of the contact also increases. For a beam and object with known geometry and material properties, the corresponding value of γ can be computed using (13). Then, for a given value of γ , the normalized half-width of the contact can be computed for a range of applied displacements using (14). The corresponding maximum contact pressure is then given by (16).

III. EXPERIMENTAL CASE STUDY

To verify the results from our mechanics models, we completed a grasping case study. A series of two-fingered, inflatable, soft Pneu-Net grippers with different stiffnesses were fabricated and the feasibility of different grasps was evaluated. For each design, we attempted to grasp a cylindrical object of a known radius and mass. If the gripper could hold the object without dropping it when pressurized to a prescribed intrinsic curvature

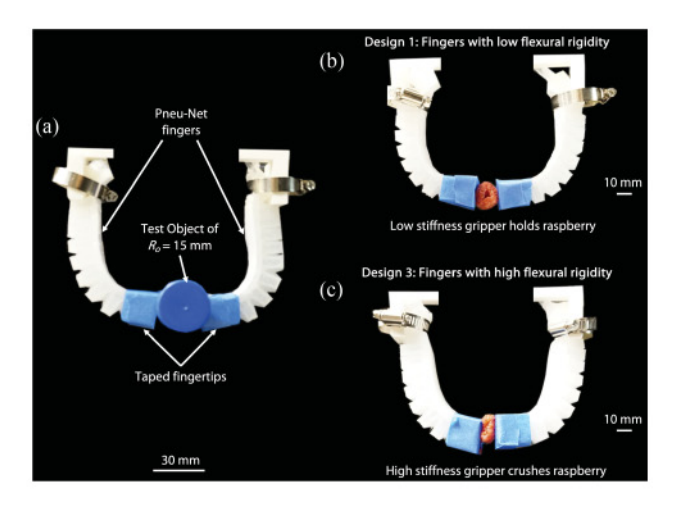


Fig. 3. (A) A two-fingered Pneu-Net gripper holding the cylindrical test object, which has a radius of 15 mm. (B) A low modulus gripper (Design 1) holding a raspberry without crushing it. (C) A high modulus gripper with increased finger thickness (Design 3) crushes the same raspberry when inflated to the same intrinsic curvature profile.

profile of $\tilde{\kappa}_0=2$, the mass was increased by 2 g, and the test was repeated until we determined the mass at which the gripper dropped the object. The maximum mass held is the load capacity. Using our model from the Theoretical Formulation & Results section, we can predict the load capacity for each design, or the mass at which the grasp becomes infeasible and moves from the blue to the orange region at a given flexural rigidity D. We fabricated four different Pneu-Net gripper designs (described below) and photos of example grasps are given in Fig. 3.

We fabricated a control (1) using a low-modulus elastomer (Ecoflex 00-30, Smooth-On Inc.), and then increased the global stiffness by fabricating a design (2) with the same geometry, but an elastomer with higher modulus (DragonSkin 10 A FAST, Smooth-On Inc.). To demonstrate the impact of geometry-based changes to flexural rigidity, we fabricated a third design (3) comprised of the higher modulus elastomer with increased base thickness. Finally, to demonstrate the effect of a non-uniform interface modulus, we built (4) a gripper with a high modulus body and a low modulus fingertip. We measured the load capacity of each design for a cylindrical object with $R_o = 15 \text{ mm}$ at a fixed contact location of $\beta = 0$, fixed gripper separation S, and fixed gripper height H for all grasps. Each fingertip and test object was wrapped in tape to ensure a clean and uniform interface, and we measured the static coefficient of friction to be $\mu = 0.4$ for a tape/tape contact. Thus, we used feasibility bounds of $\mu_{min} < 0.4$ and N < 2.2 N in our model for this case study, which represented the actual coefficient of friction of the contact and the normal force required to dent the test object (approximately 10× the object's weight). All Pneu-Net actuators use the design from [25] with a total length of 100 mm and eleven inflatable chambers with a wall thickness of 2 mm. The control base thickness is 4 mm (Designs 1, 2, 4) and 8 mm for Design 3. For each actuator, a pre-cut piece of paper serves as the inextensible layer. The measured load capacities for Designs 1, 2, 3, and 4 were 32 g, 36 g, 50 g, and 52 g, respectively.

IV. DISCUSSION

A. Grasp Feasibility: Effect of Gripper Flexural Rigidity

From the analysis of gripper stiffness on grasp feasibility, it is apparent that changes in a finger's flexural rigidity have a significant impact on grasp feasibility. Overall, a larger flexural rigidity results in larger normal forces at the contact location (Fig. 4B), which reduces the minimum friction coefficient required for a successful grasp at the majority of contact locations. For any particular grasping scenario where one gripper is to be used to pick up a variety of objects, one must consider the ability of the objects to withstand normal force without damage. After doing so, one can properly select the maximum degree of global stiffness change the gripper should undergo to successfully and safely lift all objects without applying too much normal force at the selected contact locations.

B. Grasp Feasibility: Effect of Object Mass

Increased object masses greatly reduce the feasible region for grasp success for grippers with lower flexural rigidity, as there is insufficient normal force generated to satisfy the constraint on the allowable coefficient of friction, as seen in Fig.5A, C. In other words, the coefficient of friction in these scenarios would have to be unreasonably large for a successful grasp of a heavy object to take place. Next, increases in object mass over the range examined do not greatly change the size of the feasible region for grippers with increased stiffness, as the increase in object mass does not cause a significant reduction in the normal force generated at the contact. In this scenario, the gripper is sufficiently stiff to deflect minimally under large object loads. Grippers with a reduced flexural rigidity are good for gentle grasping of delicate objects (Fig.3B) or human-robot interaction tasks [19], but gripper stiffness should be increased to increase load capacity. Therefore, a gripper with tunable stiffness could achieve both of these functions in one device, moving from a soft state to ensure low normal forces to avoid object damage, and then to a stiff one to successfully lift. Such tunable stiffness materials would increase the gripper's versatility, or the number of objects it could successfully grasp.

C. Grasp Feasibility: Effect of Object Radius

Our analysis shows that object size also has an effect on grasp success. First, the normal force generated at a contact correlates with the total deflection of the fingertip with respect to the finger's intrinsic curvature profile κ_0 . For the gripper design parameters we selected for the grasp feasibility plot in Fig.5 B, the gripper deflection is largest for the objects with smaller R_o , resulting in larger normal forces (Fig.4C). As the object size increases, the amount of fingertip deflection relative to the finger's intrinsic curvature profile also decreases. Thus, the normal force begins to drop as object size increases. The minimum required coefficient of friction follows the opposite trend of the normal force, since $\mu \geq F_{fr}/N$. If other design parameters including κ_0 and S all vary, the trends we observed with changing object size will also change, as the gripper's initial curvature and position relative to the object impact the

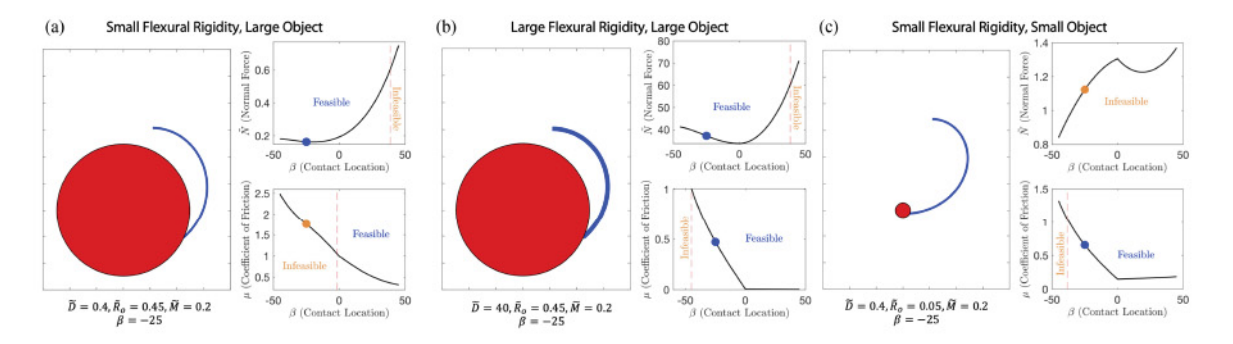


Fig. 4. Visualizations of different grasp configurations with grasp feasibility conditions applied. Plots of \tilde{N} vs. β and μ vs. β for different grasps. The feasible and infeasible regions are noted on each plot, and the black line indicates the \tilde{N} and μ values computed from (2) for $\beta=-45$ to 45. A marker is colored blue or orange if the grasp associated with those parameters is feasible or infeasible for $\beta=-25$. (a) A gripper with reduced flexural rigidity $\tilde{D}=0.4$ contacting a large object of radius $\tilde{R_o}=0.45$ with mass $\tilde{M}=0.2$. We use the N<0.1 N boundary to determine grasp feasibility based on N for this case. (b) A gripper with increased flexural rigidity $\tilde{D}=40$ contacting a large object of radius $\tilde{R_o}=0.45$ with mass $\tilde{M}=0.2$. We use the N<10 N boundary to determine grasp feasibility based on N for this case. (c) A gripper with reduced flexural rigidity $\tilde{D}=0.4$ contacting a small object of radius $\tilde{R_o}=0.05$ with mass $\tilde{M}=0.2$. We use the N<0.1 N boundary to determine grasp feasibility based on N for this case.

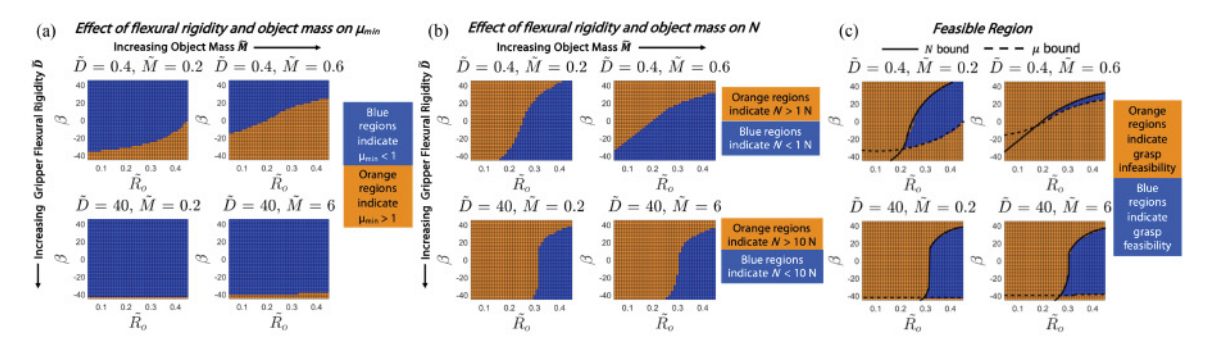


Fig. 5. Results showing the effect of stiffness on grasp feasibility for the configuration shown in Fig.1. (a) The effect of finger flexural rigidity on the minimum required coefficient of friction at different contact locations β for objects of varying size $\tilde{R_o}$ and half-mass \tilde{M} . (b) The effect of finger flexural rigidity on the normal force generated at different contact locations β for objects of varying size $\tilde{R_o}$ and half-mass \tilde{M} . (c) The effect of finger flexural rigidity and contact location on grasp feasibility.

final amount of fingertip deflection and normal force generated. While the results suggest that changes in S, gripper angle, or κ_0 should lead to similar feasibility trends which result from changes in R_o , this is an area for future work.

D. Grasp Feasibility: Effect of Contact Location

Our analysis demonstrates that grasp feasibility has a complex dependence on the contact location β . This arises due to the fact that β affects both the normal force generated and the friction required to lift the object. For $\beta > 0$, adhesive interactions aid in lifting the object, while for β < 0, the normal force contributes to the total grasping force. As β varies in these two regimes, the normal force output also varies. As such, it is the relative rate at which normal force and the required frictional force vary as a function of β that determines grasp feasibility. This variation is complex and, as can be seen from our results, is also highly dependent on D, M, and R_o . For larger contact areas resulting from either additional fingertip contacts (e.g., for a four-fingered gripper) or contact along the length of the fingers (i.e., wrapping of the object), the contribution of adhesion will be more significant. Furthermore, as $\beta \to 90$, the gripper must rely on adhesion to lift the object. This suggests that, when designing

a gripper, one must consider objects and operating conditions for which grasping cannot be achieved using only friction. For these scenarios (e.g., flat, low profile objects, objects in a bin with limited lateral space, etc.), the gripper should be designed to have sufficient adhesion strength.

E. Contact Area and Pressure: Effect of Stiffness

From the analysis of contact between a deformable gripper and object, it is clear that the geometry and elastic properties of both the gripper and object affect the contact area and pressure at the interface. In general, larger contact areas and lower contact pressures are desired for grasping to increase lifting capacity while preventing damage to the object. As shown in Fig. 6, an increase in the ratio E_g/E^* results in an increase in contact area. Therefore, assuming a constant object modulus, the contact area can be increased by increasing the gripper modulus. However, increasing the gripper modulus also increases the contact modulus and, thus, the maximum contact pressure as suggested by (16). To avoid this increase in contact pressure while still increasing the contact area, stiffer material can be added away from the contact to increase the effective gripper modulus without changing the contact modulus.

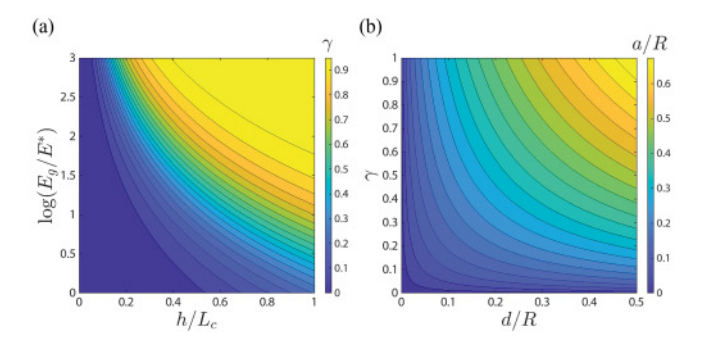


Fig. 6. (a) The fraction γ of the applied displacement d resulting in bulk deformation in the vicinity of the contact plotted as a function of the non-dimensional parameters E_g/E^* and h/L_c . (b) The normalized contact half-width a/R plotted as function of the fraction γ and the normalized displacement d/R.

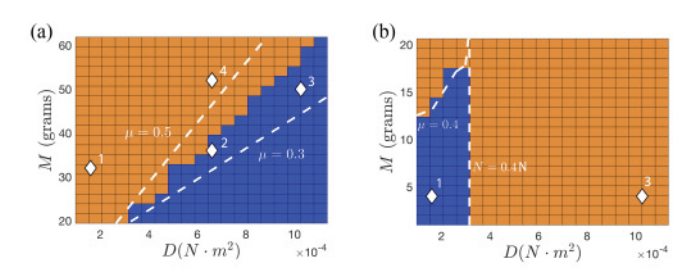


Fig. 7. (a) Flexural rigidity D vs. object mass M for a rigid test object ($R_o=15$ mm, S=53 mm, $\beta=0$, $\tilde{\kappa_0}=2$), with the load capacity results for four finger designs presented as white data points. Each data point is labeled with its corresponding finger design. Each dotted line indicates a ± 0.1 deviation from the $\mu=0.4$ boundary (all designs satisfied the N condition). (b) Flexural rigidity D vs. object mass M for a delicate test object ($R_o=8.5$ mm, S=53 mm, $\beta=0$, $\tilde{\kappa_0}=2$), with the load capacity results for two finger designs presented as white data points. The data point associated with Design 1 led to a successful grasp with no damage (Fig. 3B), while the data point associated with Design 3 led to a grasp where the object was damaged (Fig. 3C).

F. Contact Area and Pressure: Effect of Geometry

Fig. 6 also shows that an increase in h/L_c results in an increase in contact area. In other words, the contact area increases as the gripper gets thicker and as the contact occurs closer to the clamped end. For a thin gripper with contact occurring far from the clamped end, the beam is compliant because of its geometry and the contact forces act over a large moment arm, which results in greater beam deflection. This results in smaller contact area and, thus, lower contact pressure. Furthermore, the contact area and pressure are less sensitive to the applied displacement. Therefore, for a gripper of a given thickness, positioning the object further from the clamped end can be useful when handling fragile objects. Meanwhile, for a thick gripper with contact occurring close to the clamped end, there is larger contact area and higher pressure, with both increasing more quickly with increasing displacement. Therefore, positioning the object closer to the clamped end can help with handling larger, heavier objects.

G. Grasp Feasibility: Experimental Case Study

Fig. 7A shows a plot of flexural rigidity vs. object mass for our fixed set of experimental conditions and a rigid test object $(R_o = 15 \text{ mm}, S = 53 \text{ mm}, \beta = 0, \tilde{\kappa_0} = 2)$, with the load capacity results for the four finger designs shown as labeled data points (white diamonds). We apply feasibility conditions of $\mu_{min} < 0.4$ and N < 2.2 N to generate the feasible/infeasible regions. Since we measured the load capacity of each design, we expected each data point to fall on the boundary between the feasible/infeasible regions. For the high modulus finger designs (Designs 2 & 3), we found that the load capacity results fell very close to the feasibility boundary predicted by the model. This is an improvement compared to existing grasping force models for soft grippers based on Cosserat theory [26]. We also found that a reduction in contact modulus from an added fingertip of low-modulus (Design 4) led to an increase in load capacity, which our grasp feasibility model could not directly capture. This phenomenon also occurred for the homogeneous, low-modulus fingers (Design 1). This result, while highlighting a limitation of our model, aligned with our analysis from Fig. 6, which indicates that a softer contact modulus should lead to increased contact areas and higher load capacities. Thus, we have demonstrated that stiffness both at the contact and away from the contact can be designed to increase gripper performance.

Next, we confirmed the effect of stiffness on load capacity performance. First, increasing the flexural rigidity of the Pneu-Net finger by increasing its modulus alone led to an increase in force capacity (Design 1 vs. Design 2). Furthermore, increasing the flexural rigidity via geometric changes led to a further increase in force capacity (Design 2 vs. Design 3). However, by adding a reduced modulus fingertip to our high modulus finger, we were able to increase force capacity without changing the actuator geometry (Design 2 vs. Design 4). These results demonstrate (i) that there are numerous design options to change the flexural rigidity of a finger, either by modifying its materials composition and/or geometry and (ii) our modeling approach is a useful tool for quantifying the effects of these changes on grasp feasibility.

We also tested a grasping scenario with a delicate object (a 4 g raspberry), as seen in Fig. 3B and 3C. We first grasped the raspberry without damage using our low-modulus design (Design 1). However, when we switched to a design with larger flexural rigidity (Design 3) and inflated the gripper to the same intrinsic curvature profile, we damaged the raspberry. Using feasibility conditions of $\mu_{min} < 0.4$ and N < 0.4 N, where the N bound corresponds to $10\times$ the mass of one raspberry, the model was able to predict a feasible grasp for Design 1 and an infeasible grasp for Design 3, which we show in Fig. 7B. In all, we have demonstrated that certain finger designs with different flexural rigidities could require unattainable amounts of friction for a successful grasp, or result in normal forces which damage the object, which our feasibility conditions account for.

V. LIMITATIONS & FUTURE WORK

The presented model for determining grasp feasibility is limited to a two-dimensional analysis that only allows for planar configurations and deformation of the end effector. Moreover,

grasp feasibility is assessed only on a gripper's ability to provide sufficient lifting force. The model does not consider the effect of out-of-plane bending and twisting of the gripper's fingers or object rotations that could lead to grasp instability. While this is an important consideration for future work, the goal of this work was to provide guidance regarding the selection of gripper material modulus (either static or tunable) and geometry to provide sufficient lifting force without object damage assuming a stable grasp configuration. While we only consider the grasping of cylindrical objects, the results and intuition from our work should apply to non-cylindrical objects. We also note that our model assumes force closure grasps [24], as opposed to form closure, or enveloping grasps. Future work also includes an investigation of the effect of stiffness selection for these caging scenarios, where contact is made between gripper and object at locations other than the fingertip. While we consider a two-fingered gripper and a cylindrical object for simplicity and brevity, the intuition provided by the analysis can be used to guide the design of grippers with more than two fingers and non-cylindrical objects. The lifting force provided by each finger on a multi-fingered gripper can be determined by solving (2) for each finger separately. Other future investigations of interest include studies of multi-fingered grasps (with more than two fingers), changes in object shape, changes in the horizontal distance between gripper and object, changes in gripper angle, and non-uniform stiffness distributions.

VI. CONCLUSION

In this work, we have presented a mechanics-based investigation for designing versatile grippers based on stiffness considerations. We presented models to quantify the effect of stiffness on the ability of different grippers to form contact and how different types of gripping forces, including frictional, normal, and adhesive interactions, can be leveraged and controlled. We provided quantitative conditions for grasp feasibility, which, in conjunction with our models, provide guidelines for gripper design. From the results of our models and experimental case study, it is clear that all three forces must be considered when designing a gripping system, and that changes in finger stiffness both far and close to a contact will affect grasp success in terms of contact area and contact force generation. Thus, our investigation demonstrates that stiffness is a key variable in gripper design and that materials with tunable material properties offer potential for extending the range of objects that one gripper can successfully grasp and lift.

REFERENCES

- S. Zaidi, M. Maselli, C. Laschi, and M. Cianchetti, "Actuation technologies for soft robot grippers and manipulators: A review," *Curr. Robot. Rep.*, vol. 2, no. 3, pp. 355–369, 2021.
- [2] J. Shintake, V. Cacucciolo, D. Floreano, and H. Shea, "Soft robotic grippers," Adv. Mater., vol. 30, no. 29, 2018, Art. no. 1707035.

- [3] K. W. O'Brien et al., "Elastomeric passive transmission for autonomous force-velocity adaptation applied to 3D-printed prosthetics," Sci. Robot., vol. 3, no. 23, 2018, Art. no. eaau5543.
- [4] H. Lipson, "Challenges and opportunities for design, simulation, and fabrication of soft robots," Soft Robot., vol. 1, no. 1, pp. 21–27, 2014.
- [5] A. M. Dollar and R. D. Howe, "Towards grasping in unstructured environments: Optimization of grasper compliance and configuration," in *Proc.* IEEE/RSJ Int. Conf. Intell. Robots Syst., 2003, vol. 4, pp. 3410–3416.
- [6] A. Dollar and R. Howe, "Joint coupling design of underactuated grippers," in *Proc. Int. Des. Eng. Tech. Conf. Comput. Inf. Eng. Conf.*, 2006, vol. 42568, pp. 903–911.
- [7] J. Hughes, U. Culha, F. Giardina, F. Guenther, A. Rosendo, and F. Iida, "Soft manipulators and grippers: A review," Front. Robot. AI, vol. 3, 2016, Art. no. 69.
- [8] D. J. Levine, K. T. Turner, and J. H. Pikul, "Materials with electroprogrammable stiffness," Adv. Mater., vol. 33, no. 35, 2021, Art. no. 2007952.
- [9] M. Manti, V. Cacucciolo, and M. Cianchetti, "Stiffening in soft robotics: A review of the state of the art," *IEEE Robot. Automat. Mag.*, vol. 23, no. 3, pp. 93–106, Sep. 2016.
- [10] L. Wang et al., "Controllable and reversible tuning of material rigidity for robot applications," Mater. Today, vol. 21, no. 5, pp. 563–576, 2018.
- [11] J. Shintake, B. Schubert, S. Rosset, H. Shea, and D. Floreano, "Variable stiffness actuator for soft robotics using dielectric elastomer and lowmelting-point alloy," in *Proc. IEEE/RSJ Int. Conf. Intell. Robots Syst.*, 2015, pp. 1097–1102.
- [12] M. Tatari, A. M. Nasab, K. T. Turner, and W. Shan, "Dynamically tunable dry adhesion via subsurface stiffness modulation," *Adv. Mater. Interfaces*, vol. 5, no. 18, 2018, Art. no. 1800321.
- [13] R. Coulson, C. J. Stabile, K. T. Turner, and C. Majidi, "Versatile soft robot gripper enabled by stiffness and adhesion tuning via thermoplastic composite," *Soft Robot.*, 2021, doi: 10.1089/soro.2020.0088.
- [14] H. Imamura, K. Kadooka, and M. Taya, "A variable stiffness dielectric elastomer actuator based on electrostatic chucking," *Soft Matter*, vol. 13, no. 18, pp. 3440–3448, 2017.
- [15] J. R. Amend, E. Brown, N. Rodenberg, H. M. Jaeger, and H. Lipson, "A positive pressure universal gripper based on the jamming of granular material," *IEEE Trans. Robot.*, vol. 28, no. 2, pp. 341–350, Apr. 2012.
- [16] C. B. Teeple, T. N. Koutros, M. A. Graule, and R. J. Wood, "Multi-segment soft robotic fingers enable robust precision grasping," *Int. J. Robot. Res.*, vol. 39, no. 14, pp. 1647–1667, 2020.
- [17] X. Zhou, C. Majidi, and O. M. O'Reilly, "Soft hands: An analysis of some gripping mechanisms in soft robot design," *Int. J. Solids Struct.*, vol. 64, pp. 155–165, 2015.
- [18] K. L. Johnson, K. Kendall, and A. Roberts, "Surface energy and the contact of elastic solids," *Proc. Roy. Soc. London. A. Math. Phys. Sci.*, vol. 324, no. 1558, pp. 301–313, 1971.
- [19] H. Yuk, S. Lin, C. Ma, M. Takaffoli, N. X. Fang, and X. Zhao, "Hydraulic hydrogel actuators and robots optically and sonically camouflaged in water," *Nature Commun.*, vol. 8, no. 1, pp. 1–12, 2017.
- [20] M. Duduta, E. Hajiesmaili, H. Zhao, R. J. Wood, and D. R. Clarke, "Realizing the potential of dielectric elastomer artificial muscles," *Proc. Nat. Acad. Sci.*, vol. 116, no. 7, pp. 2476–2481, 2019.
- [21] J. Li, F. Zhou, and X. Wang, "Modify the friction between steel ball and PDMS disk under water lubrication by surface texturing," *Meccanica*, vol. 46, no. 3, pp. 499–507, Jun. 2010.
- [22] I. Kao and C. Ngo, "Properties of the grasp stiffness matrix and conservative control strategies," *Int. J. Robot. Res.*, vol. 18, no. 2, pp. 159–167, 1999.
- [23] H. Dong, C. Qiu, D. K. Prasad, Y. Pan, J. Dai, and I.-M. Chen, "Enabling grasp action: Generalized quality evaluation of grasp stability via contact stiffness from contact mechanics insight," *Mechanism Mach. Theory*, vol. 134, pp. 625–644, 2019.
- [24] V.-D. Nguyen, "Constructing force-closure grasps," Int. J. Robot. Res., vol. 7, no. 3, pp. 3–16, 1988.
- [25] B. Mosadegh et al., "Pneumatic networks for soft robotics that actuate rapidly," Adv. Funct. Mater., vol. 24, no. 15, pp. 2163–2170, 2014.
- [26] Y. Haibin, K. Cheng, L. Junfeng, and Y. Guilin, "Modeling of grasping force for a soft robotic gripper with variable stiffness," *Mechanism Mach. Theory*, vol. 128, pp. 254–274, 2018.